JOC Article
pubs.acs.org/joc

Kinetic Evidence for Dihapto (η^2) π-Aryl Participation in Acid-Catalyzed Ring Opening of Diarylhomobenzoquinone Epoxides

Haruyasu Asahara, Kohta Saito, Naohiko Ikuma, and Takumi Oshima*

Department of Applied Chemistry, Graduate School of Engineering, Osaka University, 2-1 Yamadaoka, Suita, Osaka 565-0871, Japan

oshima@chem.eng.osaka-u.ac.jp

Received October 19, 2009

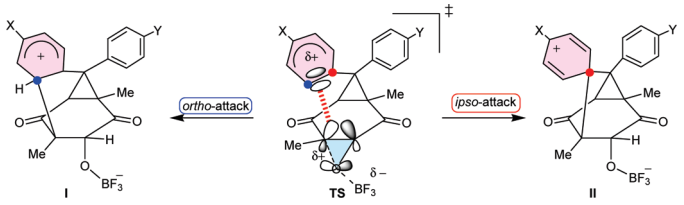

The BF_3-catalyzed ring-opening reaction of variously *endo*/*exo* *m*- and *p*-substituted diarylhomobenzoquinone epoxides proceeded through a transannular S_E2-Ar cyclization of *endo*-aryl groups to give the tricyclic diketo-alcohols and cyclohexadienone spiro-linked tricyclic diketo-alcohols. Kinetics of these reactions has been investigated in $CDCl_3$ at 30 °C in order to elucidate the possible remote π-aryl participation. The rates were significantly increased with increasing electron-donating ability of the *endo*-aryl substituents X ($k^{p\text{-MeO}}/k^{p\text{-CF3}} = 8200$) but only negligibly influenced by the distal *exo*-aryl substituents Y ($k^{p\text{-MeO}}/k^{p\text{-CF3}} = 2.1$). For the *endo*-X substituted series, an excellent linear free energy relationship, $\log k_{rel}^{endo} = -2.49\sigma^{ipso} - 1.62\sigma^{ortho} - 0.108$ ($R^2 = 0.98$, $n = 8$), was attained using two modified site-dependent substituent parameters σ^{ipso} (using σ_p^+ for *p*-X and σ_m for *m*-X) and σ^{ortho} (using σ_m for *p*-X and σ_p^+ for *m*-X). This means that the dihapto(η^2) π-coordination occurs in the π-aryl participation, with the *ipso* π-electron donation contributing 1.6 times more effectively than the *ortho* one. On the other hand, the distal *exo*-Y substituted series gave an acceptable Yukawa−Tsuno equation with small polar and resonance contributions; $\log k_{rel}^{exo} = -0.912(\sigma^0 + 0.237\Delta\bar{\sigma}_R^+)$ ($R^2 = 0.96$, $n = 8$). These kinetic substituent effects were compared with those of the acid-catalyzed π-aryl assisted transannular S_E2-Ar cyclization of the cyclobutene-fused diarylhomobenzoquinones. It was found that the geometrical characteristics of the vacant oxirane Walsh orbital and the cyclobutene antibonding orbital play a crucial role in the topological features of η^2 π-aryl participation.

Introduction

π-Aryl participation is one of the most sophisticated physicochemical phenomena that control the reactivity of substrates and sometimes govern the reaction mechanism.[1] These effects are generally derived from (ascribed to) the through-space electronic stabilization of the transition states by the direct π-electronic donation (not by resonance) from the contained aryl groups to the reaction center (usually but not necessarily an incipient carbocation).[2] A large number of studies have been made of the π-aryl-assisted solvolyses of β-aryltosylates and brosylates from the kinetic[3] and stereochemical[4] point of view. In these adjacent β-aryl-substituted substrates, the kinetic substituent effects as well as the

(1) (a) Lancelot, C. J.; Cram, D. J.; Scheyer, P. v. R. *Carbenium Ions*; Olah, G. A., Scheyer, P. v. R., Eds.; Wiley-Interscience: New York, 1972; Vol. 3, Chapter 27, pp 1347−1483. (b) Smith, M. B.; March, J. *March's Advanced Organic Chemistry*; Wiley: New York, 2007; Chapter 11, pp 657−751. (c) Peeran, M. J.; Wilt, W.; Subramanian, R.; Crumrine, D. S. *J. Org. Chem.* **1993**, *58*, 202–210. (d) Kevil, D. N.; D'Souza, M. J. *J. Chem. Soc., Perkin Trans. 2* **1997**, 257–263. (e) Fujio, M.; Goto, N.; Dairokuno, T.; Goto, M.; Saeki, Y.; Okusaka, Y.; Tsuno, Y. *Bull. Chem. Soc. Jpn.* **1992**, *65*, 3072–3079. (f) Nagumo, S.; Ono, M.; Kakimoto, Y.; Furukawa, T.; Hisano, T.; Mizukami, M.; Kawahara, N.; Akita, H. *J. Org. Chem.* **2002**, *67*, 6618–6622. (g) del Río, E.; Menéndez, M. I.; López, R.; Sordo, T. *J. Am. Chem. Soc.* **2001**, *123*, 5064–5068.

(2) Isaacs, N. S. *Physical Organic Chemistry*; Longman Science & Technical: Essex, 1995; Chapter 13, pp 643−700.

(3) (a) Fujio, M.; Funatsu, K.; Goto, M.; Mishima, M.; Tsuno, Y. *Tetrahedron* **1987**, *43*, 307–316. (b) Fujio, M.; Goto, M.; Mishima, M.; Tsuno, Y. *Bull. Chem. Soc. Jpn.* **1990**, *63*, 1121–1128. (c) Okamura, M.; Hazama, K.; Ohta, M.; Kato, K.; Horaguchi, T.; Ohno, A. *Chem. Lett.* **1997**, *26*, 973–974. (d) Tsuno, Y.; Fujino, M. *Advances in Physical Organic Chemistry*; Bethell, D., Ed.; Academic Press: London, 1999; Vol. 32, pp 267−385.

(4) (a) Cram, D. J. *J. Am. Chem. Soc.* **1952**, *74*, 2129–2137. (b) Cram, D. J. *J. Am. Chem. Soc.* **1952**, *74*, 2137–2148. (c) Streitwieser, A., Jr.; Walsh, T. D.; Wolfe, J. R. *J. Am. Chem. Soc.* **1965**, *87*, 3686–3691. (d) Cram, D. J.; Thompson, J. A. *J. Am. Chem. Soc.* **1967**, *89*, 6766–6768. (e) Thompson, J. A.; Cram, D. J. *J. Am. Chem. Soc.* **1969**, *91*, 1778–1789.

DOI: 10.1021/jo902179x Published on Web 12/21/2009

SCHEME 1

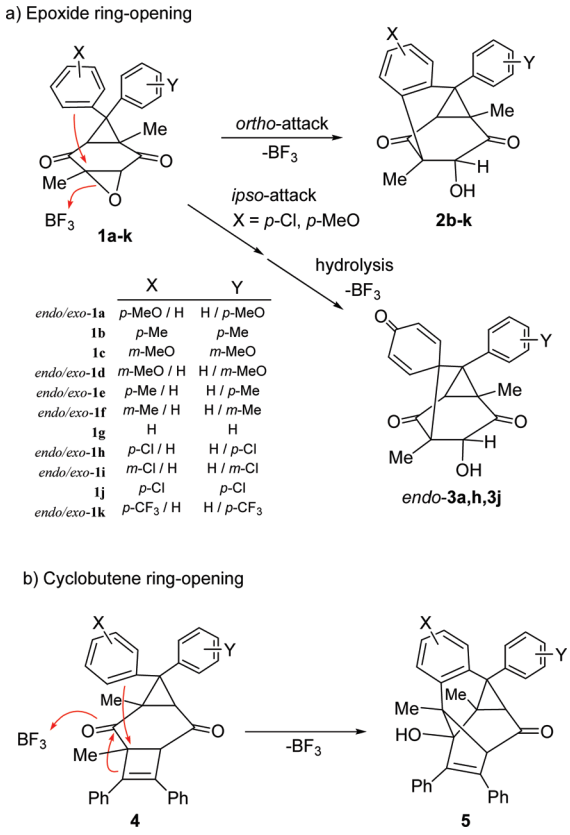

product analyses clearly indicated that the π-aryl participation occurs at the proximal *ipso*-carbon and hence the phenonium ion (σ-complex) can be formed as an intermediate. By contrast, little is known for the anchimeric assistance of the aryl group located in the γ-position or further away from the reaction site.[5] However, the remote π-aryl participation is of continuous theoretical interest because a detailed understanding of the physical origin and scope of such interactions has become one of the major goals of physical organic chemistry. Compared to the more conventional π-aryl participation at the *ipso*-position, the elucidation of the steric and electronic factors controlling the remote electron-donation and knowing which positions of the aromatic ring are responsible for such phenomenon are of prime importance.

Very recently, we reported that the unsubstituted and *p*-substituted diphenylhomobenzoquinone epoxides **1** (X, Y = H, Me, and Cl) show a remote π-aryl participated transannular S_E2-Ar cyclization of *endo*-phenyl group associated with the acid-catalyzed regioselective oxirane ring cleavage to give the *ortho*-carbon bound tricyclic diketo-alcohols **2** and the *ipso*-carbon bound 2,5-cyclohexadien-4-one spiro-linked tricyclic diketo-alcohol **3** (only for the π-resonating *p*-Cl substituted entity) as shown in Scheme 1a.[6] This observation raises a question as to which positions of the aromatic ring and how the aryl group interacts with the vacant oxirane Walsh orbital.[7]

Herein, aiming at obtaining physicochemical information on the π-aryl participated transition state, we have conducted kinetic studies of the BF_3-catalyzed transannular cyclization of variously *endo*/*exo m*- and *p*-substituted diarylhomobenzoquinone epoxides **1a**−**k** in $CDCl_3$ at 30 °C. On the basis of the kinetic substituent effects, we have found that the dihapto (η^2)-type coordination (through *ipso* and *ortho*) of the *endo*-aromatic ring occurs in the rate-determining oxirane ring cleavage. A modified Hammett treatment indicated that the *ipso*/*ortho* contribution ratio (1.6) is considerably higher than that (0.89) of the similar S_E2-Ar transannular cyclization of cyclobutene-fused diarylhomobenzoquinones **4** into the *ortho*-carbon bound tetracyclic keto-alcohols **5** (Scheme 1b).[8] These results were explained in terms of the stereoelectronic effects in the orbital interaction between the π-donor aromatic rings (HOMO) and the vacant *anti*-bonding orbitals of the cleaved oxirane and cyclobutene rings (LUMO).

Results and Discussion

Synthesis and Structural Characteristics of Epoxides. The *endo*/*exo*-substituted diarylhomobenzoquinone epoxides **1a**−**k** were prepared by the epoxidation of diarylhomobenzoquinones[9] derived from 1,3-dipolar cycloaddition of the corresponding *m*- and *p*-substituted diphenyldiazomethanes with 2,5-dimethyl-1,4-benzoquinone.[10] For the monosubstituted diphenyldiazomethanes, a mixture of *endo*/*exo*-substituted isomers was formed and separated by careful column chromatography and recrystallization. The *m*-chloro-substituted *endo*/*exo*-**1i**, however, could not be isolated due to the very similar *endo*/*exo* adsorbability on silicagel. The structures of **1a**−**k** were deduced as the *cis-transoid-cis* tricyclic dione frame from the representative X-ray crystal structural analysis of bis(*p*-chlorophenyl)-substituted **1j** (Figure 1).[11] The original quinone frame was found to adopt an appreciable pseudoboat conformation with a slight deformation opposite to the *endo*-aromatic ring. This deformation results in an overhang of *endo*-aryl ring above the quinone plane and a pseudoaxial flipping of the conjunct planar oxirane ring as noted by the average dihedral angle (95.4°) between the epoxide ring and the fused quinone plane. The very short spatial distance (3.21 Å) between the *endo*-aromatic *ipso*-carbon and the cleaved epoxide tertiary carbon seems to allow the π-electron donation to the underlying acid-activated oxirane ring. However, the corresponding distance (4.74 Å) with the outside *exo*-aromatic *ipso*-carbon is long enough to inhibit the through-space π-electron donation. Such π-electron participation becomes very important if the

(5) (a) Jackman, L. M.; Haddon, V. R. *J. Am. Chem. Soc.* **1974**, *96*, 5130–5138. (b) Gates, M.; Frank, D. L.; Felten, W. C. *J. Am. Chem. Soc.* **1974**, *96*, 5138–5143. (c) Ando, T.; Yamawaki, J.; Saito, Y. *Bull. Chem. Soc. Jpn.* **1978**, *51*, 219–224.

(6) Oshima, T.; Asahara, H.; Koizumi, T.; Miyamoto, S. *Chem. Commun.* **2008**, *15*, 1804–1806.

(7) (a) Mollere, P. D.; Houk, K. N. *J. Am. Chem. Soc.* **1977**, *99*, 3226–3333. (b) Iwamura, H.; Sugawara, T.; Kawada, Y.; Tori, K.; Muneyuki, R.; Noyori, R. *Tetrahedron Lett.* **1979**, *20*, 3449–3452. (c) Bach, R. D.; Wolber, G. J. *J. Am. Chem. Soc.* **1984**, *106*, 1410–1415.

(8) Koizumi, T.; Harada, K.; Mochizuki, E.; Kokubo, K.; Oshima, T. *Org. Lett.* **2004**, *6*, 4081–4084.

(9) Miyashita, M.; Suzuki, T.; Yoshikoshi, A. *Chem. Lett.* **1987**, 285–288.

(10) Oshima, T.; Nagai, T. *Bull. Chem. Soc. Jpn.* **1988**, *61*, 2507–2512.

(11) Crystallographic data for this compound have been deposited at the Cambridge Crystallographic Data Centre. These data can be obtained free of charge via www.ccdc.cam.ac.uk/data-request/cif, by emailing data_request@ccdc.cam.ac.uk, or by contacting The Cambridge Crystallographic Data Centre, 12 Union Road, Cambridge CB2 1EZ, U.K.; fax: +44 1223336033. CCDC 749514.

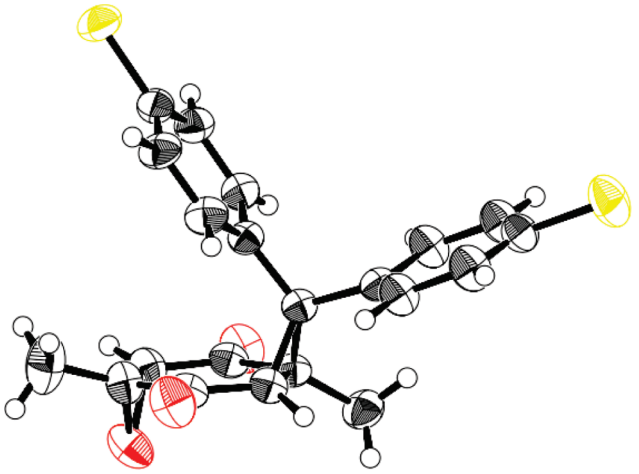

FIGURE 1. ORTEP drawing of bis(*p*-chlorophenyl) homobenzoquinone epoxide **1j** with 50% ellipsoid probability.

present epoxide ring-opening reaction proceeds through an S_N2-type intramolecular transannular cyclization. As a result, the geometrical features of **1** can take advantage of π-anchimeric assistance in the present acid-catalyzed ring opening.

Kinetic Substituent Effects. The observed pseudo-first-order rate constants k_{obs}(**1**) were divided by the concentration of BF_3 to provide the second-order rate constants k(**1**). The values for k(**1**) and the relative rate constants k_{rel}(**1**) (vs the unsubstituted **1g**) are collected in Table 1. For comparison, Table 1 also includes the relative rate constants k_{rel}(**4**) (vs the unsubstituted entity) for the previous BF_3-catalyzed reactions of similarly *endo*/*exo* *m*- and *p*-substituted analogous cyclobutene-fused diarylhomobenzoquinones **4a**−**k**.[8]

A perusal survey of Table 1 indicated some noticeable differences between the epoxides **1a**−**k** and the cyclobutene-fused **4a**−**k**: (1) for the *endo*-substituted series, the rates were increased more effectively in **1** ($k^{p\text{-MeO}}/k^{p\text{-CF3}} = 8200$) than in **4** (5600);[12] (2) by contrast, the same substituent change brought about only a small increase for the *exo*-substituted **1** (2-fold) and for **4** (11-fold); (3) of particular interest is that the *endo*-*p*-substituted **1** (X = MeO, Me, Cl) reacted faster than the *endo*-*m*-substituted isomer, whereas the *endo*-*m*-substituted **4** exhibited reactivity rather higher than that of the *endo*-*p*-substituted isomer; (4) on the other hand, *exo*-*m*/*p*-substituted couples showed the usual substituent effects for both **1** and **4**.

Since the *endo*-aromatic ring is located at the δ-position with respect to the epoxide carbon atom, the notable rate-acceleration by electron-donating *m*- and *p*-substituents can not be ascribed to direct induction or the resonance stabilization of a rate-determining transition state. Indeed, the *exo*-aromatic substituents lacked drastic effects on the rates. Accordingly, the remarkable rate dependency on the *endo*-substituents must be explained by considering the through-space electron donation of the overhanging aromatic nucleus

TABLE 1. Rate Constants k and Relative Rate Ratios k_{rel}(1**) for BF_3-Catalyzed Rearrangements of 1 and Relative Rate Ratios k_{rel}(**4**) for the Reaction of 4 in $CDCl_3$ at 30°C**

		substituent				
entry	compound	X	Y	$10^3 \times k$(**1**)[a], $M^{-1}\ s^{-1}$	k_{rel}(**1**)	k_{rel}(**4**)[b]
1	*endo*-**1a**	*p*-MeO	H	18.7	37	17
2	**1b**	*p*-Me	*p*-Me	5.25	11	5.3
3	**1c**	*m*-MeO	*m*-MeO	3.90	8.0	
4	*endo*-**1d**	*m*-MeO	H	3.70	7.6	22
5	*endo*-**1e**	*p*-Me	H	3.11	6.4	4.9
6	*endo*-**1f**	*m*-Me	H	1.36	2.8	5.6
7	**1g**	H	H	0.486	1.0	1.0[c]
8	*endo*-**1h**	*p*-Cl	H	0.122	0.25	0.017
9	*endo*-**1i**	*m*-Cl	H	0.0213	0.044	0.078
10	**1j**	*p*-Cl	*p*-Cl	0.0154	0.032	0.015
11	*endo*-**1k**	*p*-CF_3	H	0.00217	0.0045	0.0040
12	*exo*-**1a**	H	*p*-MeO	0.602	1.2	3.2
13	*exo*-**1d**	H	*m*-MeO	0.456	0.94	0.94
14	*exo*-**1e**	H	*p*-Me	0.523	1.1	1.2
15	*exo*-**1f**	H	*m*-Me	0.478	0.98	0.70
16	*exo*-**1h**	H	*p*-Cl	0.420	0.86	0.39
17	*exo*-**1i**	H	*m*-Cl	0.345	0.71	0.33
18	*exo*-**1k**	H	*p*-CF_3	0.278	0.57	0.30

[a]The second-order rate constants k were obtained by dividing the pseudo-first-order rate constant k_{obs} by the concentration of BF_3. The k values are the average of at least two measurements. Error limit of k is ±2%. [b]The relative rate constant of cyclobutene ring-opening reaction of analogous homobenzoquinones **4**. [c]The second-order rate constant k(**4g**) $= 1.25 \times 10^{-3}\ M^{-1}\ s^{-1}$ (cf ref 8).

to the acid-activated oxirane ring. In order to evaluate the degree to which the present acid-catalyzed ring-opening reactions respond to the *meta* and *para* substituent changes of **1**, we applied a linear free energy relationships analysis for k_{rel}(**1**). As a consequence, it was found that the usual Hammett treatment for the *endo*-X substituted series by using σ or σ^+ single parameter[13] provided rather poor correlations; $\log k_{rel}^{endo}(\mathbf{1}) = -4.5\sigma + 0.35$ ($r^2 = 0.89$, $n = 8$) and $-2.8\sigma^+ - 0.09$ ($r^2 = 0.77$, $n = 8$) respectively.[14] These unsatisfactory correlations with the normal single parameter are suggestive of π-aryl participation of the *endo*-aromatic ring not only at the *ipso*- but also at the *ortho*-carbon atom. This simultaneous binding seems to be responsible for the formation of the *ortho*- and the *ipso*-carbon bound products, **2j** and **3j**, from the bis(*p*-chlorophenyl)-substituted **1j** (Scheme 1a).[6]

On the basis of these findings, we thought that the transannular S_E2-Ar cyclization of *endo*-aryl groups of **1** involves a dihapto (η^2) π-aryl participated transition state through the *ipso*- and the *ortho*-carbon atom. Although the *m*-substituted aromatic nucleus has two different *ortho*-positions with respect to the *ipso*-carbon, the less congested *ortho*-position, that is to say *para* to the introduced *m*-substituent, is expected to participate in the product formation (vide infra). Accordingly, we attempted to correlate the $\log k_{rel}^{endo}$(**1**) with the combination of newly defined two site-dependent substituent parameters σ^{ipso} and σ^{ortho}, which display the substituent effects on the *ipso*- and *ortho*-aromatic carbon atoms, respectively. Thus, the substituent

(12) Our attempt to follow the rate of the reaction of di(*p*-anisyl)-homobenzoquinone epoxide by NMR failed because of the very fast degradation. Interestingly, this reaction gave neither **2**- nor **3**-type product but yielded di(anisyl)methyl-substituted benzoquinone derivative **6**, which seems to arise from the cyclopropane ring cleavage as well as the loss of oxygen atom. The structure of **6** was determined by the X-ray crystal structural analysis (see Supporting Information). CCDC 750112.

(13) Williams, A. *Free Energy Relationships in Organic and Bio-organic Chemistry*; The Royal Society of Chemistry: Cambridge, 2003.

(14) We obtained rather worse correlations when we assumed the π-aryl participation occurs only at the *ortho*-carbon; $\log k_{rel}exo(\mathbf{1}) = -0.38\sigma - 0.01$ ($R^2 = 0.96$, $n = 8$) and $-0.24\sigma^+ - 0.05$ ($R^2 = 0.82$, $n = 8$).

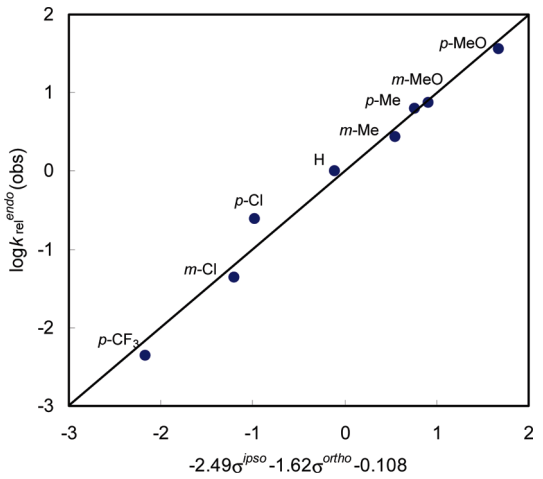

FIGURE 2. Plots of the observed log k_{rel}^{endo}(**1**)(obs) vs the calculated log k_{rel}^{endo}(**1**)(calc) according to eq 1 for BF_3-catalyzed rearrangements of unsubstituted **1g** and *endo*-substituted **1a, d-f, h, i**, and **k** in $CDCl_3$ at 30 °C.

constant σ^{ipso} is related to the *ipso*-participation by using σ_p^+ for *p*-X and σ_m for *m*-X substituent.[13] On the other hand, the other σ^{ortho} refers to the *ortho*-participation by using, specifically, σ_m for *p*-X and σ_p^+ for the *m*-X substituent, respectively. As expected, a very sufficient regression was obtained by considering such η^2-type coordination of the *endo*-aromatic ring through the *ipso*- and *ortho*-positions (eq 1 and Figure 2). Here, it is noteworthy that the η^2-binding of the aromatic ring is more effectively performed at the *ipso*-carbon than the *ortho* as indicated by the percent contribution of the parameter σ^{ipso} (61%) and σ^{ortho} (39%).

$$\log k_{rel}^{endo}(\mathbf{1}) = -2.49\sigma^{ipso} - 1.62\sigma^{ortho} - 0.108 \quad (R^2 = 0.98,\ n = 8) \tag{1}$$

As to the *exo*-Y substituted series, we observed only 2-fold rate acceleration irrespective of the wide range of *p*-MeO/*p*-CF_3 substituent variation. These *exo*-isomers provided a good linear free energy relationship when we used the Yukawa−Tsuno (Y-T) equation,[15,3d] where σ^0 is the normal substituent constant and $\Delta\bar{\sigma}_R^+$ is the resonance substituent constant defined by ($\sigma^+ - \sigma^0$) (eq 2). The present reaction yielded a small negative reaction constant ($\rho = -0.912$) and a small resonance parameter ($r = 0.237$). These very low values are certainly due to the reduced *exo*-substituent effects on the far more remote acid-activated oxirane ring (δ-position through the intervened cyclopropane and carbonyl function). Incidentally, the well-known acetolyses of β-aryltosylates and brosylates at 75−115 °C also displayed the Y-T equations with larger ρ values of −3.3 to −4.0 and *r* values of 0.54−0.63.[16] The enhanced substituent effects of these reactions can be explained by the formation of phenonium ion intermediates via the π-aryl participation at the *ipso*-carbon.

$$\log k_{rel}^{exo} = -0.912(\sigma^0 + 0.237\Delta\bar{\sigma}_R^+) \quad (R^2 = 0.96,\ n = 8) \tag{2}$$

In the following section, we will discuss these kinetic substituent effects from a mechanistic viewpoint in comparison with those of the analogous S_E2-Ar transannular cyclization of **4a**−**k**.

Mechanistic Considerations. (1). π-Aryl Participation in S_N2-Type Ring Opening of Epoxide. The acid-catalyzed cleavage of the oxirane C−O bond preferentially occurs in such a way that the substituent of the oxirane ring further stabilizes the developing positive charge by both electron donation and conjugation.[17] Accordingly, the reaction features are highly dependent on the substituents on the oxirane ring as well as the nucleophiles. Mechanistically, the nucleophilic displacement of epoxides can be rationalized by either concerted attack of a nucleophile on the acid-activated oxirane ring (S_N2 mechanism) or by stepwise attack of a nucleophile on a preformed carbocation intermediate (S_N1 mechanism).[17b,e,18] Most of the reactions are generally known to proceed through the regio- and stereoselective ring cleavage under S_N2 anti nucleophilic assistance.[19] However, the S_N1 mechanism is reported for the reaction of epoxides bearing strongly electron-releasing and conjugated substituents in highly polar solvents.[20]

Since the present epoxide ring is substituted by two electron-withdrawing quinone carbonyl groups, the acid-catalyzed ring cleavage of **1** seems to obey the S_N2 process in the less polar $CDCl_3$.[21] Under these conditions, the overhanging *endo*-aromatic ring is apt to behave as an effective internal π-nucleophile. Indeed, we have obtained very poor kinetic solvent effects ($k^{dichloroethane}/k^{benzene} = 3.0$) regardless of the appreciable change of solvent polarity (as indicated by the polarity parameter; $E_T(30)$ = 41.3 for 1,2-dichloroethane and 34.3 for benzene)[22] for the same transannular cyclization of **1g** by protic acid $MeSO_3H$.[6] The negligible solvent effects can be taken as a conclusive mechanistic criterion for the concerted process involving the less polar transition state.[21]

The mechanistic evidence for the concertedness was also obtained for the above-mentioned dual *ipso*/*ortho* transannular S_E2-Ar reactions of bis(*p*-chlorophenyl)homobenzoquinone epoxide **1j**.[6] The common π-aryl participated

(15) (a) Yukawa, Y.; Tsuno, Y. *Bull. Chem. Soc. Jpn.* **1959**, *32*, 971–981. (b) Shorter, J. *Correlation Analysis in Chemistry. Recent Advances*; Chapman, N. B., Shorter, J., Eds.; Plenum Press: New York, 1978; Chapter 4, pp 119−173.

(16) (a) Fujio, M.; Funatsu, K.; Goto, M.; Mishima, M.; Tsuno, Y. *Tetrahedron* **1987**, *43*, 307–316. (b) Fujio, M.; Goto, M.; Mishima, M.; Tsuno, Y. *Bull. Chem. Soc. Jpn.* **1990**, *63*, 1121–1128. (c) Fujio, M.; Goto, N.; Dairokuno, T.; Goto, M.; Saeki, Y.; Okusako, Y.; Tsuno, Y. *Bull. Chem. Soc. Jpn.* **1992**, *65*, 3072–3079.

(17) (a) Parker, R. E.; Issaacs, N. S. *Chem. Rev.* **1959**, *59*, 737–799. (b) Rickborn, B. In *Comprehensive Organic Synthesis*; Trost, B. M., Ed.; Pergamon Press: Oxford, U.K., 1991; Vol. 3, pp 733−771. (c) Fujita, H.; Yoshida, Y.; Kita, Y. *Yuki Gosei Kagaku Kyokaishi*. **2003**, *61*, 133–143. (d) Giner, J.-L.; Li, X.; Mullins, J. J. *J. Org. Chem.* **2003**, *68*, 10079–10086. (e) Whalen, D. E. *Advances in Physical Organic Chemistry*; Richard, J. P. Ed.; Elsevier Academic Press: London, 2005; Vol. 40, pp 247−298.

(18) *Aziridines and Epoxides in Organic Synthesis*; Yudin, K. A. Ed.; Wiley-VCH: Weinheim, 2006.

(19) (a) Posner, G. H.; Rogers, D. Z. *J. Am. Chem. Soc.* **1977**, *99*, 8214–8218. (b) Bellucci, G.; Berti, G.; Ingrosso, G.; Mastrorilli, E. *J. Org. Chem.* **1980**, *45*, 299–303.

(20) (a) Pocker, Y.; Ronald, B. P. *J. Am. Chem. Soc.* **1980**, *102*, 5311–5316. (b) Yagi, H.; Jerina, D. M. *J. Org. Chem.* **2007**, *72*, 9983–9990. (c) Davis, C. E.; Bailey, J. L.; Lockner, J. W.; Coates, R. M. *J. Org. Chem.* **2003**, *68*, 75–82. (d) Blumenstein, J. J.; Ukachukwu, V. C.; Mohan, R. S.; Whalen, D. L. *J. Org. Chem.* **1993**, *58*, 924–932.

(21) Reichart, C. *Solvents and Solvent Effects in Organic Chemistry*, 3rd ed.; Wiley-VCH Verlag GmbH & Co. KGaA: Weinheim, 2003; Chapter 5, pp 162−199.

(22) Reichardt, C. *Chem. Rev.* **1994**, *94*, 2319–2358.

SCHEME 2

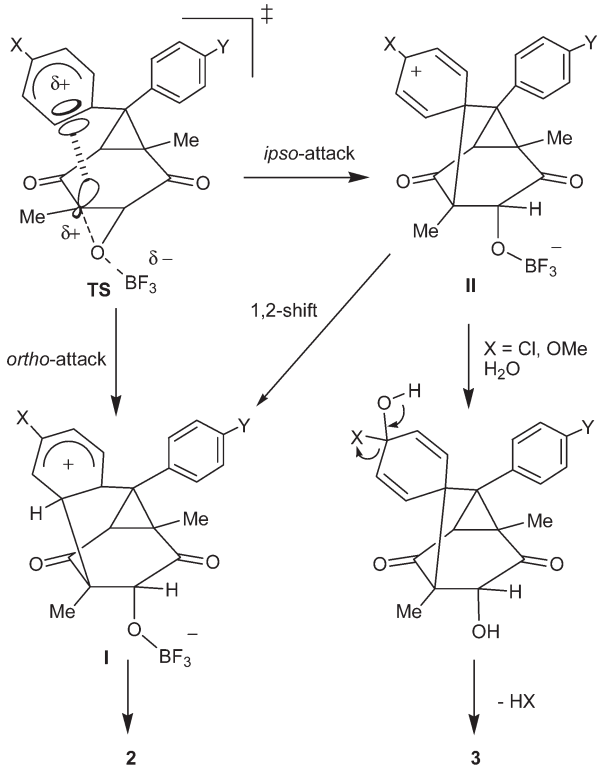

transition state leads to the *ortho*-linked product **2** via σ-complex **I** and competitively to the *ipso*-linked product **3** via the π-resonating σ-complex **II** followed by the hydrolysis with residual water (Scheme 2). The present *p*-anisyl- and *p*-chloro-substituted *endo*-**1a** and *endo*-**1h** also provided **3a** (~100%) and **3h** (80%) along with **2h** (20%), respectively. Quantitative and high yield formation of compounds **3** for the reaction of *endo*-**1a** and *endo*-**1h** (including *p*,*p*′-Cl substituted **1j**) may be explained in view of the reaction pathways on which the common transition state TS would undergo the very facile degradation into the π-resonating and water-sensitive intermediate **II** rather than the less stabilized **I**. By contrast, other *para*-substituents brought about the exclusive formation of **2** via the *ortho*-linked σ-complex **I**. This is probably because the possible *ipso*-linked σ-complex **II** cannot be transformed into the stable **3** via the nucleophilic displacement by residual water but rather undergoes a facile 1,2-shift to the *ortho*-linked **I** leading to **2**. Thus, it is not suprising that the percent contribution of the σ^{ipso} and σ^{ortho} in the transition state stabilization cannot be directly reflected on the product distributions, which are dependent on the following channels to the respective **I** and **II** as well as the contaminant water. We also found that the transannular cyclization of the *endo m*-X-substituted aromatic ring occurs exclusively at the less congested *ortho*-position (i.e., *para*-position with respect to the *m*-X) as confirmed by the representative reaction of *endo m*-MeO-substituted **1d**. A significant steric hindrance of *m*-MeO with the oxirane Me group probably inhibits the alternative π-aryl participation at the adjacent *ortho*-position.

(2). Prominent Role of Oxirane Walsh Orbital. In the acid-catalyzed intramolecular S_E2-Ar reactions of **1a**−**k**, the vacant oxirane Walsh orbital seems to play a crucial role in the initial epoxide ring opening with the aid of the *endo*-aromatic ring.[23] However, the aryl participation in the ring opening of epoxides is scarcely reported but has been put forward in the acid-induced ring opening of a particular case of epoxides bearing aryl groups directly or indirectly linked to the oxirane ring. For instance, the well-documented phenonium ion intermediates via the aryl participated transition states are invoked in the reactions of stilbene oxides[17a] and spiro-linked 2-phenyl-1,2-epoxide[24] or 1-benzyl-1,2-epoxides.[25] In our previous study using the ethano-bridged diphenylhomobenzoquinone epoxides, we have found that the rate of the acid-catalyzed transannular cyclization is highly dependent on the rigid conformation of the *endo*-aryl ring.[23] We rationalized the conformational effects on the basis of the π-aryl participated orbital interaction with the vacant oxirane Walsh orbital. Keeping this in mind, we will later interpret the present kinetic substituent effects in terms of the geometrically restricted orbital interaction in the S_N2-type epoxide ring opening.

We have previously found that the analogous cyclobutene-fused *endo*/*exo m*- and *p*-substituted diarylhomobenzoquinones **4** exhibited the similar π-aryl participated transannular S_E2-Ar cyclization under BF_3 acid conditions (Scheme 1b).[6] This cyclobutene ring-opening reaction involves a formal vinyl-anion migration to the adjacent acid-activated carbonyl carbon associated with the concerted S_N2 transannular cyclization of *endo*-aryl group.[26] Accordingly, the vacant cyclobutene *anti*-bonding orbital activated by the adjoining BF_3-complexed carbonyl group will accept the π-electrons of the *endo*-aryl group and facilitate the σ-bond cleavage. Therefore, a comparison between the epoxide and the cyclobutene ring-opening reactions will provide a very useful insight into the stereoelectronic effects in the π-aryl participated orbital interaction.

Stereoelectronic Effects in Dihapto(η^2) π-Aryl Participation. As previously reported, we have obtained an excellent two parameter regression using the σ^{ipso} and σ^{ortho} parameters for the BF_3-catalyzed transannular cyclization of cyclobutene-fused *endo m*- and *p*-substituted diarylhomobenzoquinones **4** (eq 3).[6] This equation also manifested η^2-coordination in the π-aryl participated transition state (Figure 3b). The percent contribution of σ^{ipso} (47%) is slightly smaller than that of σ^{ortho} (53%). This is in contrast to the reaction of epoxides **1**, where the σ^{ipso} contributed 1.6 times more effectively than σ^{ortho} (eq 1).

$$\log k_{rel}{}^{endo}(\mathbf{4}) = -2.07\sigma^{ipso} - 2.33\sigma^{ortho} - 0.172 \quad (R^2 = 0.99,\ n = 8) \qquad (3)$$

Why does *endo*-**4** undergo slightly enhanced substituent effects on the *ortho*-carbon atom, but in *endo*-**1** the more

(23) Oshima, T.; Asahara, H.; Kubo, E.; Miyamoto, S.; Togaya, K. *Org. Lett*. **2008**, *10*, 2413–2416.

(24) Kita, Y.; Furukawa, A.; Futamura, J.; Higuchi, K.; Ueda, K.; Fujioka, H. *Tetrahedron* **2001**, *57*, 815–825.

(25) (a) Costantino, P.; Crotti, P.; Ferretti, M.; Macchia, F. *J. Org. Chem.* **1982**, *47*, 2917. (b) Crotti, P.; Ferretti, M.; Macchia, F.; Stoppioni, A. *J. Org. Chem*. **1984**, *49*, 4706–4711. (c) Crotti, P.; Ferretti, M.; Macchia, F.; Stoppioni, A. *J. Org. Chem*. **1986**, *51*, 2759–2766.

(26) Recently, Wang and Tantillo suggested a stepwise reaction pathway for the acid-catalyzed transannular cyclization of **4** based on DFT calculations: Wang, S. C.; Tantillo, D. J. *J. Org. Chem*. **2007**, *72*, 8394–8401. However, the poor kinetic solvent effects for the reaction of **4** and especially for the present **1** explicitly rule out the intervention of the carbocation intermediate derived from the stepwise S_N1 mechanism.

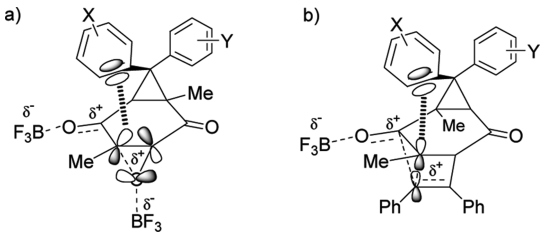

FIGURE 3. (a) Representative lowest unoccupied Walsh orbital of epoxides **1**. (b) Unoccupied orbital (in part) of cyclobutene ring of **4**.

significant substituent effects are on the *ipso*-carbon atom? To answer this question, we must recall that the acid-catalyzed S_N2-type nucleophilic displacement of **1** and **4** involves the π-aryl participated transition states. The π-electron donation should occur onto the vacant oxirane Walsh orbital of **1** and the cyclobutene antibonding σ^* orbital of **4**, respectively. Since the lowest unoccupied Walsh orbital (LUMO) is trigonally bent, the geometrical orbital interaction with the *endo*-aromatic ring (HOMO) may be represented in Figure 3. Thus, the dihapto π-aryl participation of **1** can be more effectively performed at the *ipso*-carbon rather than the *ortho*-one (Figure 3a). By contrast, such a stereoelectronic preference for the *ipso*-position should be considerably reduced for **4** because the vector of the relevant four-membered cyclobutene σ^*-bond deviates from the vertical plane through the *ipso*- and *para*-position of the aromatic ring (Figure 3b). Indeed, a theoretical calculation by the DFT B3LYP/6-31G* method[27] apparently showed the similar geometrical characteristics for the relevant vacant orbitals of epoxide and cyclobutene ring moieties (Figure 4). The vacant Walsh orbital of **1g** at the carbon corner is conjugated with the carbonyl π^*-orbital but is rather directed to the aromatic *ipso*-carbon (as yellow dotted arrow in Figure 4a). On the other hand, the vector of the vacant cyclobutene orbital of **4g** is essentially perpendicular (yellow dotted arrow) to the quinone plane and is expected to enjoy the ideal *ipso*/*ortho* η^2 coordination with the faced *endo*-aromatic nucleus (Figure 4b). This is because the epoxides **1g** display more effective *ipso*-contribution in the η^2 π-aryl participation than the cyclobutene-cleaved **4g**.

As to the *exo*-Y substituted **4**, we previously obtained the Y-T equation (eq 4) with a larger r value of 0.904 compared with that of the similar equation for *exo*-**1** (r = 0.237, eq 2).[6] The larger resonance parameter r means that the π-delocalization of *exo*-aryl substituents of **4** can appreciably stabilize the developing positive charge on the acid-activated γ-located carbonyl carbon atom. Such an activation of the carbonyl π^*-orbital results in the acceleration of the concerted vinyl anion migration responsible for the S_E2-Ar transannular cyclization of **4**. By contrast, as seen in Y-T eq 2, the reduced resonance stabilization by the *exo*-aryl substituents of **1** may be due to the change in the reaction mechanism. The epoxide ring opening is substantially facilitated by the binding of BF_3 not at the carbonyl oxygen but at the epoxide oxygen atom. Even if the carbonyl function is activated by BF_3 as in **4**, it would rather deactivate the ring opening because of the destabilization of the developing positive charge on the epoxide carbon atom.

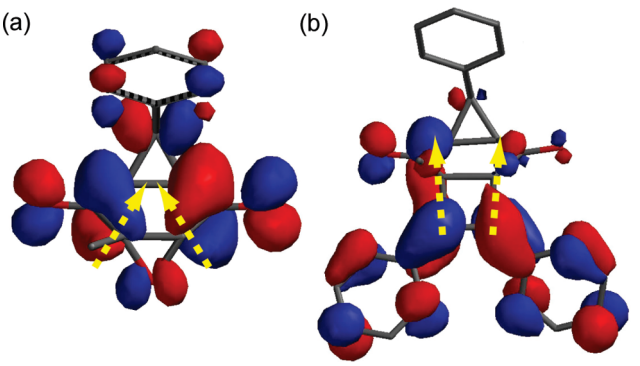

FIGURE 4. LUMO orbitals of (a) epoxide **1g** and (b) cyclobutene-fused analogue **4g** optimized by B3LYP/6-31G* method (*exo*-aromatic ring is omitted for clarity).

$$\log k_{\mathrm{rel}}{}^{exo} = -0.794(\sigma^0 + 0.904\Delta\bar{\sigma}_R{}^+) \; (R^2 = 0.96, n = 8) \quad (4)$$

Conclusion

In summary, we have performed a kinetic study of the BF_3-catalyzed ring-opening reactions of *endo*/*exo* *m*- and *p*-substituted diarylhomobenzoquinone epoxides **1**. These reactions proceeded through two types of S_E2-Ar transannular cyclizations to give tricyclic diketo-alcohols and cyclohexadienone spiro-linked tricyclic diketo-alcohols, respectively. The rates were significantly accelerated by the through-space π-aryl participation of electron-donating *endo*-aromatic rings but negligibly influenced by the through-bond electronic effects of *exo*-aromatic rings. The Hammett treatment using modified site-dependent substituent parameters σ^{ipso} and σ^{ortho} indicated that the *ipso*/*ortho* dihapto(η^2) π-aryl participation occurs for the *endo*-aryl groups. Kinetics substituent effects of these reactions were compared with those of the analogous acid-catalyzed transannular cyclization of the cyclobutene-fused diarylhomobenzoquinones **4**. It was found that the present epoxides **1** exhibit the η^2 π-aryl participation with 1.6-times more effective contribution at the *ipso*-position, whereas the cyclobutene-fused homologues **4** show almost comparable *ipso*/*ortho* contribution. These results were interpreted in terms of the geometrical features of the π-electron accepting vacant orbital of oxirane and the cyclobutene ring. The physicochemical information obtained in the present study will provide very important insight into the understanding of the π-aryl participation as well as mechanistic aspects in the acid-catalyzed ring-opening reaction of epoxides.

Experimental Section

Materials. Deuterated chloroform ($CDCl_3$) was purchased from Aldrich Chemicals Ltd. and used without further purification. All epoxides **1a**−**k** were prepared according to the previous methods by the epoxidation of the corresponding diarylhomobenzoquinones.[6] The *endo*/*exo* isomeric mixtures were separated by column chromatography on silica gel with a mixture

(27) Kong, J.; White, C. A.; Krylov, A. I.; Sherrill, D.; Adamson, R. D.; Furlani, T. R.; Lee, M. S.; Lee, A. M.; Gwaltney, S. R.; Adams, T. R.; Ochsenfeld, C.; Gilbert, A. T. B.; Kedziora, G. S.; Rassolov, V. A.; Maurice, D. R.; Nair, N.; Shao, Y. H.; Besley, N. A.; Maslen, P. E.; Dombroski, J. P.; Daschel, H.; Zhang, W. M.; Korambath, P. P.; Baker, J.; Byrd, E. F. C.; Van, Voorhis, T.; Oumi, M.; Hirata, S.; Hsu, C. P.; Ishikawa, N.; Florian, J.; Warshel, A.; Johnson, B. G.; Gill, P. M. W.; Head-Gordon, M.; Pople, J. A. *J. Comput. Chem.* **2000**, *21*, 1532–1548.

of hexane/ethyl ether as an eluent and purified by recrystallization from chloroform/pentane. The analytical data are collected below. Unfortunately, we could not obtain the pure *endo*-**1e**, *endo*/*exo*-**1i** because of contamination of the respective isomers. The assignment of the *endo*/*exo* stereochemistry of **1a**, **d**−**f**, **h**, and **k** failed because of the complexity in their ^{1}H NMR spectra. Thus, the stereochemistry was tentatively deduced from their kinetic behaviors, i.e., the more reactive isomers of **1a** and **d**−**f** are *endo*, but the more reactive isomers of **1h**, **i**, and **k** are *exo*.

Kinetic Measurements. The kinetic data were obtained by at least duplicate measurements according to the NMR spectroscopic methods. The solution of epoxide **1** (0.02 mmol) in $CDCl_3$ (0.67 mL) for kinetic experiments was prepared in a stoppered NMR tube and preheated at 30 °C (±0.1) in a thermostatted bath. The reaction was initiated by the quick addition of the requisite volume of catalyst $BF_3\cdot OEt_2$ (0.30 M) by a microsyringe and submitted for the NMR measurements in a thermostatted tube holder at 30 °C (±0.1). The introduced amount of $BF_3\cdot OEt_2$ was reduced to 1/10 and 1/5 for the reactive **1a** and increased to 3 times for the least reactive *endo*-**1k**. The NMR tubes for the less reactive *endo*-**1i**, **1j**, and for the least reactive *endo*-**1k** were sealed with a gas burner. The progress of reactions was followed at requisite time intervals by monitoring the relative signal intensity of the diagnostic methy groups on cyclopropane (0.91−1.01 ppm) and oxirane ring (1.17−1.22) of **1** over 75% conversion with respect to the internal standard TMS. For *endo*-**1i**, **1j**, and *endo*-**1k**, the measurements were performed by taking the sealed NMR tube out of the thermostatted bath (30 ± 0.1 °C). The logarithmic plots of the relative amounts of **1** with respect to the amount at the measurement starting point ($t = 0$) versus time gave a straight line. The obtained first-order rate constants k_{obs} were divided by the concentration of catalyst to provide the second-order rate constants k. The first-order decay plots and the logarithmic plots for the most reactive *endo*-**1a**, the reference **1g**, and the least reactive *endo*-**1k** are represented in Supporting Information.

Acid-Catalyzed Reaction of 1a−k. The acid-induced reactions of epoxides **1a**−**k** (0.02 mmol) were carried out in the presence of $BF_3\cdot OEt_2$ (0.40 mmol) in $CDCl_3$ (0.67 mL) at room temperature. After completion of the reactions, the reaction solution was transferred into a separate funnel, diluted with chloroform (10 mL), and then washed with water (3 mL × 3). The aqueous layer was extracted with chloroform (5 mL × 2). The combined organic layer was washed with water (3 mL × 3) and then dried over calcium chloride. After the evaporation of the solvent in vacuo, the residue was submitted for the ^{1}H NMR analysis to determine the product distributions. The reactions were found to give the *ortho*-carbon bound tricyclic diketo-alcohols **2b**−**k** together with the *ipso*-carbon bound 2,5-cyclohexadien-4-one spiro-linked tricyclic diketo-alcohol **3a** (∼100%), **3h** (the same as **3a**, 80%), and **3j** (81%) for *endo*- **1a**, *endo*-**1h**, and **1j**, respectively, in almost quantitative total yields based on the consumed **1**. Except for the representative reactions of *endo*-**1a**, **1b**, *endo*-**1d**, *endo*-**1h**, and **1j**, no further detailed analyses of products were carried out. The analytical data of the products **2b**, **2g**, **2j**, and **3j** have been already described elsewhere.[6,28] The new compounds 3a and *endo*-**2d** were isolated by column chromatography on silica gel with a mixture of hexane/ethyl acetate as an eluent.

***endo*-1,5-Dimethyl-8-phenyl-8-(4-anisyl)-4-oxa-tricyclo[5.1.0.0^{3,5}]-octane-2,6-dione (*endo*-1a).** Mp 116.5−117.5 °C, colorless prisms (chloroform/pentane); ^{1}H NMR (270 MHz, $CDCl_3$) δ 0.91 (s, 3H), 1.19 (s, 3H), 2.78 (s, 1H), 2.80 (s, 1H), 3.75 (s, 3H), 6.80−6.84 (m, 2H), 7.18−7.30 (m, 7H); ^{13}C NMR (67 MHz, $CDCl_3$) δ 13.6, 16.7, 37.9, 40.0, 49.2, 55.3, 60.1, 60.4, 114.4, 127.8, 129.2, 129.5, 129.6, 132.3, 138.7, 159.0, 198.5, 200.6; IR (KBr) 1705 (C=O) cm^{-1}. Anal. Calcd for $C_{22}H_{20}O_4$: C, 75.84; H, 5.79; O, 18.37. Found: C, 75.69; H, 5.72; O, 18.59.

***exo*-1,5-Dimethyl-8-(4-anisyl)-8-phenyl-4-oxa-tricyclo[5.1.0.0^{3,5}]-octane-2,6-dione (*exo*-1a).** Mp 105.8−106.8 °C, colorless prisms (chloroform/pentane); ^{1}H NMR (270 MHz, $CDCl_3$) δ 0.99 (s, 3H), 1.17 (s, 3H), 2.79 (s, 1H), 2.86 (s, 1H), 3.73 (s, 3H), 6.76−6.79 (m, 2H), 7.16−7.37 (m, 7H); ^{13}C NMR (67 MHz, $CDCl_3$) δ 13.8, 16.8, 37.5, 39.5, 48.9, 55.3, 60.3, 60.5, 114.5, 127.5, 128.2, 129.0, 130.2, 130.8, 140.5, 159.1, 198.6, 200.8; IR (KBr) 1695 (C=O) cm^{-1}. Anal. Calcd for $C_{22}H_{20}O_4$: C, 75.84; H, 5.79; O, 18.37. Found: C, 75.69; H, 5.72; O, 18.59.

1,5-Dimethyl-8,8-ditolyl-4-oxa-tricyclo[5.1.0.0^{3,5}]octane-2,6-dione (1b). Mp 139.9−140.8 °C, colorless prisms (chloroform/pentane); ^{1}H NMR(270 MHz, $CDCl_3$) δ 0.94 (s, 3H), 1.17 (s, 3H), 2.24 (s, 3H), 2.27 (s, 3H), 2.77 (s, 1H), 2.81 (s, 1H), 7.02−7.14 (m, 6H), 7.22−7.26 (m, 2H); ^{13}C NMR (67 MHz, $CDCl_3$) δ 13.8, 16.9, 21.1, 21.1, 37.7, 39.8, 49.3, 60.1, 60.4, 128.0, 129.2, 129.5, 129.7, 135.3, 137.3, 137.3, 137.6, 198.4, 200.5; IR (KBr) 1702 (C=O) cm^{-1}. HRMS: calcd for $C_{23}H_{22}O_3$ 346.1569, found 346.1572.

1,5-Dimethyl-8,8-bis(3-anisyl)-4-oxa-tricyclo[5.1.0.0^{3,5}]octane-2,6-dione (1c). Mp 194.5−195.1 °C, colorless prisms (chloroform/pentane); ^{1}H NMR (270 MHz, $CDCl_3$) δ 0.97 (s, 3H), 1.20 (s, 3H), 2.78 (s, 1H), 2.84 (s, 1H), 3.74 (s, 3H), 3.78 (s, 3H), 6.71−7.36 (m, 8H); ^{13}C NMR (67 MHz, $CDCl_3$) δ 13.8, 16.7, 37.6, 49.5, 55.3, 60.1, 60.3, 112.7, 113.8, 114.6, 115.1, 120.7, 121.8, 130.0, 130.2, 139.5, 141.2, 159.8, 198.3, 200.5; IR (KBr) 1698 (C=O) cm^{-1}. Anal. Calcd for $C_{23}H_{22}O_5$: C, 73.00; H, 5.86; O, 21.14. Found: C, 72.97; H, 5.85; O, 21.18.

***endo*-1,5-Dimethyl-8-(3-anisyl)-8-phenyl-4-oxa-tricyclo[5.1.0.0^{3,5}]-octane-2,6-dione (*endo*-1d).** Mp 165.6−166.6 °C, colorless prisms (chloroform/pentane); ^{1}H NMR (270 MHz, $CDCl_3$) δ 0.98 (s, 3H), 1.18 (s, 3H), 2.80 (s, 1H), 2.85 (s, 1H), 3.74 (s, 3H), 6.72−6.86 (m, 3H), 7.14−7.41 (m, 6H); ^{13}C NMR (67 MHz, $CDCl_3$) δ 13.8, 16.8, 37.6, 39.7, 49.6, 55.3, 60.1, 60.3, 113.8, 115.1, 121.8, 127.7, 128.4, 128.9, 130.3, 139.6, 139.8, 159.8, 198.4, 200.5; IR (KBr) 1699 (C=O) cm^{-1}. Anal. Calcd for $C_{22}H_{20}O_4$: C, 75.84; H, 5.79; O, 18.37. Found: C, 75.72; H, 5.75; O, 18.53.

***exo*-1,5-Dimethyl-8-(3-anisyl)-8-phenyl-4-oxa-tricyclo[5.1.0.0^{3,5}]-octane-2,6-dione (*exo*-1d).** Mp 168.8−169.8 °C, colorless prisms (chloroform/pentane); ^{1}H NMR (270 MHz, $CDCl_3$) δ 0.91 (s, 3H), 1.21 (s, 3H), 2.80 (s, 1H), 2.80 (s, 1H), 3.78 (s, 3H), 6.73−6.76 (m, 1H), 6.90−6.96 (m, 2H), 7.19−7.26 (m, 6H); ^{13}C NMR (67 MHz, $CDCl_3$) δ 13.6, 16.8, 37.6, 39.7, 49.5, 55.3, 60.1, 60.4, 112.7, 114.6, 120.6, 128.0, 129.2, 129.7, 130.0, 138.2, 141.5, 159.9, 198.3, 200.6; IR (KBr) 1699 (C=O) cm^{-1}. Anal. Calcd for $C_{22}H_{20}O_4$: C, 75.84; H, 5.79; O, 18.37. Found: C, 75.72; H, 5.75; O, 18.53.

***endo*-1,5-Dimethyl-8-phenyl-8-(4-tolyl)-4-oxa-tricyclo[5.1.0.0^{3,5}]-octane-2,6-dione (*endo*-1e).** (This compound could not be obtained in pure form because of the contamination of small amount of *exo*-**1e**). ^{1}H NMR (270 MHz, $CDCl_3$) δ 0.95 (s, 3H), 1.18 (s, 3H), 2.25 (s, 3H), 2.80 (s, 1H), 2.83 (s, 1H), 7.39−6.86 (m, 3H), 7.14−7.39 (m, 9H); ^{13}C NMR (67 MHz, $CDCl_3$) δ 13.7, 16.8, 21.0, 37.5, 39.6, 49.4, 60.1, 60.4, 127.6, 128.3, 128.9, 129.4, 129.8, 135.2, 137.9, 140.3, 198.5, 200.7. Anal. Calcd for $C_{22}H_{20}O_3$: C, 79.50; H, 6.06; O, 14.44. Found: C, 79.50; H, 6.05; O, 14.45.

***exo*-1,5-Dimethyl-8-(4-tolyl)-8-phenyl-4-oxa-tricyclo[5.1.0.0^{3,5}]-octane-2,6-dione (*exo*-1e).** Mp 143.9−144.9 °C, colorless prisms (chloroform/pentane); ^{1}H NMR (270 MHz, $CDCl_3$) δ 0.91 (s, 3H), 1.19 (s, 3H), 2.28 (s, 3H), 2.79 (s, 1H), 2.80 (s, 1H), 7.10−7.28 (m, 9H); ^{13}C NMR (67 MHz, $CDCl_3$) δ 13.6, 16.8, 21.0, 37.8, 39.8, 49.5, 60.1, 60.3, 127.9, 128.2, 129.2, 129.6, 129.7, 137.1, 137.5, 138.5, 198.5, 200.7; IR (KBr) 1708 (C=O) cm^{-1}. Anal. Calcd for $C_{22}H_{20}O_3$: C, 79.50; H, 6.06; O, 14.44. Found: C, 79.50; H, 6.05; O, 14.45.

***endo*-1,5-Dimethyl-8-phenyl-8-(3-tolyl)-4-oxa-tricyclo[5.1.0.0^{3,5}]-octane-2,6-dione (*endo*-1f).** Mp 137.1−138.1 °C, colorless prisms

(28) Asahara, H.; Kubo, E.; Koizumi, T.; Mochizuki, E.; Oshima, T. *Org. Lett.* **2007**, *9*, 3421–3424.

(chloroform/pentane); ^{1}H NMR (270 MHz, $CDCl_3$) δ 0.93 (s, 3H), 1.18 (s, 3H), 2.27 (s, 3H), 2.79 (s, 1H), 2.80 (s, 1H), 6.99−7.41 (m, 9H); ^{13}C NMR (67 MHz, $CDCl_3$) δ 13.6, 16.8, 21.2, 37.6, 39.8, 49.7, 60.0, 60.2, 126.6, 127.6, 128.4, 128.7, 129.0, 129.1, 130.2, 138.2, 139.1, 140.1, 198.4, 200.5; IR (KBr) 1700 (C=O) cm^{-1}. Anal. Calcd for $C_{22}H_{20}O_3$: C, 79.50; H, 6.06; O, 14.44. Found: C, 79.33; H, 5.97; O, 14.70.

***exo*-1,5-Dimethyl-8-(3-tolyl)-8-phenyl-4-oxa-tricyclo[5.1.0.0^{3,5}]-octane-2,6-dione (*exo*-1f).** Mp 116.2−117.2 °C, colorless prisms (chloroform/pentane); ^{1}H NMR (270 MHz, $CDCl_3$) δ 0.92 (s, 3H), 1.19 (s, 3H), 2.32 (s, 3H), 2.80 (s, 1H), 2.81 (s, 1H), 7.02−7.27 (m, 9H); ^{13}C NMR (67 MHz, $CDCl_3$) δ 13.6, 16.8, 21.4, 37.6, 39.7, 49.7, 60.1, 60.3, 125.4, 127.9, 128.5, 128.8, 128.9, 129.2, 129.6, 138.4, 138.8, 139.9, 198.5, 200.7; IR (KBr) 1703 (C=O) cm^{-1}. Anal. Calcd for $C_{22}H_{20}O_3$: C, 79.50; H, 6.06; O, 14.44. Found: C, 79.33; H, 5.97; O, 14.70.

1,5-Dimethyl-8,8-diphenyl-4-oxa-tricyclo[5.1.0.0^{3,5}]octane-2,6-dione (1g). Mp 122.5−123.5 °C colorless prisms (chloroform/pentane); ^{1}H NMR (270 MHz, $CDCl_3$) δ 0.92 (s, 3H), 1.18 (s, 3H), 2.81 (s, 1H), 2.82 (s, 1H), 7.17−7.32 (m, 8H), 7.37−7.40 (m, 2H); ^{13}C NMR (67 MHz, $CDCl_3$) δ 13.7, 16.9, 37.6, 39.7, 49.6, 60.1, 60.3, 127.5, 127.9, 128.2, 128.9, 129.1, 129.5, 138.1, 139.9, 198.1, 200.3. Anal. Calcd for $C_{21}H_{18}O_3$: C, 79.22; H, 5.70; O, 15.08. Found: C, 79.10; H, 5.86; O, 15.04.

***endo*-1,5-Dimethyl-8-phenyl-8-(4-chlorophenyl)-4-oxa-tricyclo-[5.1.0.0^{3,5}]octane-2,6-dione (*endo*-1h).** Mp 126.2−127.2 °C, colorless prisms (chloroform/pentane); ^{1}H NMR (270 MHz, $CDCl_3$) δ 1.01 (s, 3H), 1.19 (s, 3H), 2.81 (s, 1H), 2.89 (s, 1H), 7.18−7.38 (m, 9H); ^{13}C NMR (67 MHz, $CDCl_3$) δ 13.6, 16.8, 37.4, 39.3, 48.3, 60.3, 60.4, 127.9, 128.3, 129.1, 129.4, 131.0, 134.2, 136.8, 139.7, 198.2, 200.5; IR (KBr) 1695 (C=O) cm^{-1}. Anal. Calcd for $C_{21}H_{17}ClO_3$: C, 71.49; H, 4.86; Cl, 10.05; O, 13.60. Found: C, 71.20; H, 4.87; Cl, 10.23; O, 13.70.

***exo*-1,5-Dimethyl-8-(4-chlorophenyl)-8-phenyl-4-oxa-tricyclo-[5.1.0.0^{3,5}]octane-2,6-dione (*exo*-1h).** Mp 173.7−174.7 °C, colorless prisms (chloroform/pentane); ^{1}H NMR (270 MHz, $CDCl_3$) δ 0.92 (s, 3H), 1.19 (s, 3H), 2.77 (s, 1H), 2.82 (s, 1H), 7.21−7.34 (m, 9H); ^{13}C NMR (67 MHz, $CDCl_3$) δ 13.6, 16.8, 37.3, 39.5, 48.6, 60.2, 60.3, 128.2, 129.2, 129.3, 129.6, 129.7, 133.7, 137.8, 138.6, 198.1, 200.3; IR (KBr) 1705 (C=O) cm^{-1}. Anal. Calcd for $C_{21}H_{17}ClO_3$: C, 71.49; H, 4.86; Cl, 10.05; O, 13.60. Found: C, 71.20; H, 4.87; Cl, 10.23; O, 13.70.

***endo*/*exo*-1,5-Dimethyl-8-phenyl-8-(3-chlorophenyl)-4-oxa-tricyclo[5.1.0.0^{3,5}]octane-2,6-dione (*endo*/*exo*-1i).** (These compounds could not be separated); ^{1}H NMR (270 MHz, $CDCl_3$) δ 0.93 (s, 3H), 1.01 (s, 3H), 1.19 (s, 3H), 1.20 (s, 3H), 2.78 (s, 1H), 2.81 (s, 1H), 2.81 (s, 1H), 2.87 (s, 1H), 7.14−7.40 (m, 18H); ^{13}C NMR (67 MHz, $CDCl_3$) δ 13.6, 13.6, 16.8, 16.8, 37.3, 37.5, 39.4, 39.5, 48.5, 48.7, 60.2, 60.2, 60.2, 60.3, 126.6, 127.8, 128.0, 128.0, 128.3, 128.3, 128.4, 128.5, 129.1, 129.3, 129.7, 129.7, 130.3, 130.5, 134.8, 135.0, 137.5, 139.3, 140.2, 141.9, 198.0, 198.0, 200.2, 200.2; IR (KBr): 1703 (C=O) cm^{-1}. Anal. Calcd for $C_{21}H_{17}ClO_3$: C, 71.49; H, 4.86; Cl, 10.05; O, 13.60. Found: C, 71.43; H, 4.83; Cl, 10.00; O, 13.74.

1,5-Dimethyl-8,8-bis(4-chlorophenyl)-4-oxa-tricyclo[5.1.0.0^{3,5}]-octane-2,6-dione (1j). Mp 142.7−143.5 °C, colorless prisms (chloroform/pentane); ^{1}H NMR(270 MHz, $CDCl_3$) δ 1.01 (s, 3H), 1.19 (s, 3H), 2.75 (s, 1H), 2.89 (s, 1H), 7.14−7.19 (m, 2H), 7.22−7.27 (m, 2H), 7.29 (s, 4H); ^{13}C NMR (67 MHz, $CDCl_3$) δ 13.8, 17.0, 37.2, 39.2, 47.4, 60.4, 129.3, 129.4, 129.6, 130.8, 133.9, 134.3, 136.1, 138.0, 197.8, 200.0; IR (KBr): 1702 (C=O) cm^{-1}. HRMS: calcd for $C_{21}H_{16}Cl_2O_3$ 386.0476, found 386.0479.

***endo*-1,5-Dimethyl-8-phenyl-8-(4-trifluoromethylphenyl)-4-oxa-tricyclo[5.1.0.0^{3,5}]octane-2,6-dione (*endo*-1k).** Mp 158.8−159.8 °C, colorless prisms (chloroform/pentane); ^{1}H NMR (270 MHz, $CDCl_3$) δ 0.96 (s, 3H), 1.22 (s, 3H), 2.85 (s, 1H), 2.87 (s, 1H), 7.24−7.55 (m, 9H); ^{13}C NMR (67 MHz, $CDCl_3$) δ 13.5, 14.0, 16.9, 37.3, 39.3, 48.4, 60.2, 60.3, 123.6 (q, J_{CF} = 272.1 Hz), 126.1 (q, J_{CF} = 3.91 Hz), 128.1, 128.4, 129.2, 130.1, 130.3 (q, J_{CF} = 33.0 Hz), 139.1, 142.3, 198.1, 200.4; IR (KBr) 1704 (C=O) cm^{-1}. Anal. Calcd for $C_{22}H_{17}F_3O_3$: C, 68.39; H, 4.43; F, 14.75; O, 12.42. Found: C, 68.27; H, 4.39; F, 14.84; O, 12.50.

***exo*-1,5-Dimethyl-8-(4-trifluoromethylphenyl)-8-phenyl-4-oxa-tricyclo[5.1.0.0^{3,5}]octane-2,6-dione (*exo*-1k).** Mp 157.8−158.8 °C, colorless prisms (chloroform/pentane); ^{1}H NMR (270 MHz, $CDCl_3$) δ 0.94 (s, 3H), 1.20 (s, 3H), 2.81 (s, 1H), 2.84 (s, 1H), 7.23−7.60 (m, 9H); ^{13}C NMR (67 MHz, $CDCl_3$) δ 13.6, 16.9, 37.1, 39.3, 48.6, 60.2, 60.3, 123.8 (q, J_{CF}=272.1 Hz), 126.1 (q, J_{CF} = 3.91 Hz), 128.4, 128.9, 129.4, 129.5 (q, J_{CF} = 33.0 Hz), 129.6, 137.3, 143.8, 197.9, 200.1; IR (KBr) 1701 (C=O) cm^{-1}. Anal. Calcd for $C_{22}H_{17}F_3O_3$: C, 68.39; H, 4.43; F, 14.75; O, 12.42. Found: C, 68.27; H, 4.39; F, 14.84; O, 12.50.

(1*R,8*R**,9*S**,10*R**,12*S**)-12-Hydroxy-5-methoxy-1,10-dimethyl-8-phenyl-tetracyclo-[6.4.1^{1,9}.0^{2,7}.0^{8,13}]trideca-2(7),3,5-triene-11,13-dione (*endo*-2d).** Mp 164.4−165.1 °C, colorless prisms (chloroform/pentane); ^{1}H NMR (270 MHz, $CDCl_3$) δ 1.14 (s, 3H), 1.24 (s, 3H), 2.63 (br, 1H), 3.05 (s, 1H), 3.58 (s, 3H), 3.65 (s, 1H), 6.06 (d, 1H, J = 2.64 Hz), 6.68 (dd, 1H, J = 2.64, 8.24 Hz), 6.97 (d, 1H, J = 8.24 Hz), 7.14−7.16 (m, 1H), 7.38−7.42 (m, 2H), 7.48−7.50 (m, 2H); ^{13}C NMR (67 MHz, $CDCl_3$) δ 14.5, 21.1, 38.2, 49.7, 54.0, 55.1, 60.6, 81.3, 112.0, 115.8, 125.0, 128.5, 128.8, 129.3, 130.1, 131.1, 136.5, 138.3, 159.6, 203.2, 205.6; IR (KBr) 3330 (−OH), 1714, 1698 (C=O) cm^{-1}. HRMS: calcd for $C_{22}H_{20}O_4$ 348.1362, found 348.1356.

Spiro[cyclohexa-2,5-dienone-4,8′-7-phenyl-1,4-dimethyl-3-hydroxy-tricyclo[2.2.2.0^{6,7}]octane-2,5-dione] 3a (same as 3h). Mp 97.3−98.1 °C, colorless prisms (chloroform/pentane); ^{1}H NMR (270 MHz, $CDCl_3$) δ 1.00 (s, 3H), 1.07 (s, 3H), 2.79 (s, 1H), 3.06 (s, 1H), 4.01 (s, 1H), 6.13 (dd, J = 1.98, 10.22 Hz), 6.51 (dd, J = 1.98, 10.22 Hz), 6.58 (dd, J = 3.30, 10.22 Hz), 6.86 (dd, J = 3.30, 10.22 Hz), 7.07 (br, 2H), 7.29 (br, 3H); ^{13}C NMR (67 MHz, $CDCl_3$) δ 10.8, 14.7, 43.2, 46.2, 53.0, 53.6, 56.0, 75.5, 128.6, 129.0, 129.2, 129.4, 131.2, 131.2, 134.2, 143.2, 148.1, 184.4, 203.7, 204.6; IR (KBr) 3411 (-OH), 1747, 1712, 1664 (C=O) cm^{-1}. HRMS: calcd for $C_{23}H_{22}O_3$ 334.1205, found 334.1197.

Acknowledgment. This work was supported by Grant-in-Aid for Scientific Research from Japan Society for the Promotion of Science (JSPS). H.A. also expresses his special thanks for The Global COE (center of excellence) program "Global Education and Research Center for Bio-Environmental Chemistry" of Osaka University.

Supporting Information Available: X-ray crystallographic data, calculation procedure, tables of atom coordinates, and full spectral data for all new compounds. This material is available free of charge via the Internet at http://pubs.acs.org.